A Novel Design of a Metacarpal/Metatarsal-Phalangeal Total Joint Replacement

Andrew Weems[1]

Abstract – Arthritis, most notably rheumatoid arthritis, can destroy the surfaces of the bones; the ideal solution for this being total joint replacement. Current total metacarpophalangeal joint replacements (TJR) do not provide the normal biomechanical range of motion and functionality. The proposed design attempts to correct this through the use design geometry and functional anatomy. Numerical analysis is used in conjunction with computational modeling to compare a one-piece silicone implant with the proposed TJR. The proposed design, due to high stress tolerances with low deformation, along with functionality and biomechanics, seems to be an appropriate replacement for the one-piece silicone implant
Keywords: Metacarpalphalangeal joints, total joint replacement, numerical analysis, computational modeling

INTRODUCTION

The joints of the fingers and the toes are identical in structure and function. The main motion of the joints is flexion and extension, with limits on the range of these movements, controlled by two major muscle groups of the same name, flexors and extensors. Extensors are on the posterior (top) of the joint and the flexors are located anteriorly. The joints of the fingers are the metacarpophalangeal (MCP or knuckle joint), the proximal interphalangeal joint (PIP) and the distal phalangeal-phalangeal joint. [1-8] In normal joints, the space between the joints is filled with cartilage that allows for smooth motion. The cartilage has a low enough coefficient of friction that the surfaces of the bones simply glide past each other. Trauma and disease can destroy or damage the cartilage between the surfaces. Cartilage is a nonvascular tissue at the center of the formation, with some blood vessels being present at the edges of the menisci; damage done to cartilage tissue is slow to heal and prone to flaws. For this reason, damage to the cartilage between joints does not resolve itself in time to be fully capable of displacing and dampening the next damaging force. Over time, the cartilage is destroyed and does not reproduce itself to replenish the surface so the trauma is applied to the surface of the bone. [9-16]

Degenerative joint disease (osteoarthritis) is the deterioration of the hyaline articulating cartilage, a dense collagen matrix that prevents loss of both functionality and material, in the synovial joint condyles. It degrades the integrity and composition of the cartilage, as a result of trauma or genetic factors. [5,9]

Arthritis, most notably rheumatoid arthritis, can destroy the surfaces of the bones.[10] These conditions remove the smooth surface of the bone as the force is applied to the joint surface. This results in the smooth surface of the joints being destroyed by repetition of the applied force from movement. As the surface heals, the joint surface is no longer frictionless and smooth; instead there are ridges and bumps that cause painful motion. Not only does motion become painful and difficult for the joint, it also causes physical disfigurement and pain even when the joint is stagnant.

There are several pain management solutions for patients with joint damage. An initial solution would be to decrease the usage of the joint. In this instance, the extremity and all the distal portions of it are no longer used. Associated issues with this method include reduced mobility and less interaction with the external environment.

[1] Mercer University, andrew.c.weems@live.mercer.edu ,andrewc.weems@yahoo.com

Another solution to managing the pain is joint fusion. The joint is crossed by a rod, effectively turning the joint into a longer, single bone. This method alleviates pain for the patient, at the cost of joint mobility. [1,2,17,18]

The ideal solution is total joint replacement (TJR), which may restore biomechanical functionality and mobility of the joint. There are limitations on current total finger and toe joint replacements in terms of stability and natural biomechanics. Current designs do not provide the normal biomechanical range of motion, which may include hyperextension/flexion of tissue or lack of proper range of motion. Additionally, the design uses incorrect materials in terms of complete biocompatibility. The bulk properties of biocompatible materials are different than those of particles. Titanium alloy is the material of choice in orthopedic implants, due to its strength and compatibility with the host environment. The bulk of the material has no adverse effects for the surrounding tissue or the host. However, after the joint is used, particulates of the alloy began to accumulate in the surrounding tissue. Over time, the concentration of the particulates increases, leading to discoloration and potential tissue damage or death. For this reason, the characteristics of the biomaterials must be examined at both the bulk and particle level, with analysis of the TJR needed prior to material selection.[1-4,10,11, 17-22]

The most common MCP and PIP replacement joint is a one-piece silicone implant that is installed via a burr hole into the medullary canal of the two bones of the joint, shown in Figure 1.[2,17,18, 3, 19, 4, 10, 23, 15, 16]

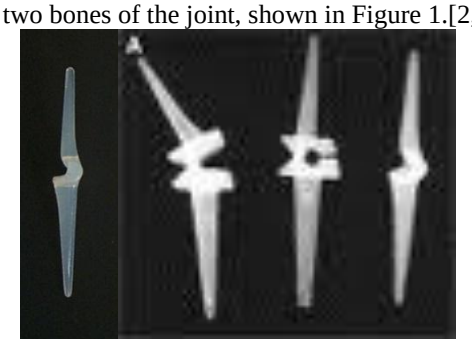

Figure 1 Examples of the one-piece silicone implant devices. [Image from Arnold-Peter Weiss, MD, Brown University]

This implant is not fixed, and as such, cannot provide the proper joint reactions to allow patients to perform basic tasks such as gripping or lifting. Additionally, concerns have been raised as to the nature of fracturing of such implants [12]. The presented total finger and toe joint implant provides all the natural biomechanics of the finger and toe joints, in addition to increased stability and durability.

METHODS AND MATERIALS

Numerical Modeling and Analysis

Current total finger and toe replacement joints were analyzed to determine the faults with each design. From this analysis, it was determined that a joint is needed that has a resistance to lateral/medial displacement, a flexion-extension range of approximately 100°, no resistance to motion and a quick installation time, in addition to biomechanical functionality. To this end, the free body diagram of the natural finger joint was analyzed in static and dynamic motion to determine the forces acting upon it, and this was then compared with the most commonly installed total metacarpophalangeal joint replacement, a one-piece silicone implant. The free body diagrams of the natural joint and the one-piece implant are shown in Figure 2.

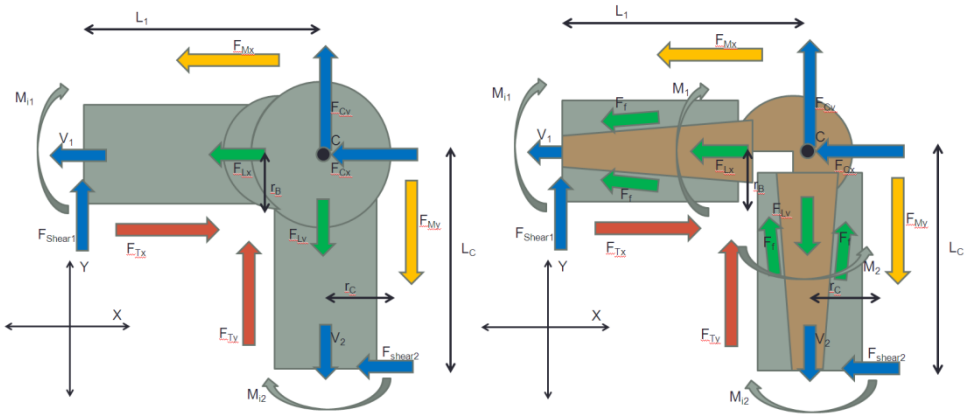

Figure 2 The free body diagrams of the natural finger joint (left) and the one-piece implant (right).

The main stabilizer tendons are shown for flexors (F_T), extensors (F_M) and the joint capsule (Fc) that holds the condyles together. For the natural finger joint, M_i is the internal moment for the bone, V is the normal force at the arbitrary slice in the diaphysis of the bone and F_{shear} is the shear force at the slice. These variables are the same for the one-piece implant, with the addition of a moment associated with the design, designated as M_1 and M_2 for the arms, respectively. This moment is due to the flexion of the arms as they are inserted into the medullary canal of the metacarpal or phalangeal bones during the surgery. The design of the joints is such that they are not fixed in the medullary canal, and are not a hinge joint. The joints were analyzed as both static and dynamic systems. The static and dynamic equations for the natural joints are shown in Equations 1-7 below

$$\sum F_x = 0 = -1[F_{shear\,2} + V_1 + F_{cx} + F_{mx} - F_{Tx} + F_{Lx}] \quad \text{(Eq 1)}$$

$$\sum F_y = 0 = F_{shear\,1} - V_2 + F_{cy} + F_{Ty} - F_{Ly} - F_{My} \quad \text{(Eq 2)}$$

$$\sum M_c = 0 = M_{i2} + M_{i1} + F_{shear\,2}(L_c) + F_{shear\,1}(L_1) - F_{Mx}r_B - F_{Tx}r_B + F_{Ty}r_c + F_{My}r_C \quad \text{(Eq 3)}$$

The condyles of the natural joint and the one-piece TJR are then solved for internal shear (shown in Eq 15, 16) which are then used to demonstrate total force values on the tendons of the digit. Additionally, it is assumed that the geometries of both bone shafts are identical.

$$F_{Ty} = \frac{-M_{i1}}{r_1}\left(\frac{L_1}{L_C} + 2\right) - \frac{M_{i2}}{r_1}\left(\frac{L_1}{L_C} + 1\right) - 2(F_{mx} + F_{Tx}) - F_{my} \quad \text{(Eq 4)}$$

$$\sum F_x = ma = -1[F_{shear\,2} + V_1 - F_{Tx} + F_{Lx} + F_{mx} + F_{jx} - F_{Ffx}] \quad \text{(Eq 5)}$$

$$\sum F_y = ma = -1[-F_{Ty} + F_{Ff} - F_{Ly} - F_{shear\,1} + V_2 + F_{jy} + F_{my} + 2m_b g] \quad \text{(Eq 6)}$$

$$\sum M_c = I\alpha = r_c\left(F_{Ty} - F_{Tx} + F_{my} - F_{mx} + F_{Ff}\cos\theta\right) - m_b g\left(\frac{L_c + L_1}{2}\right) + L_c(F_{shear\,2}) + F_{shear\,1}(L_c) - M_{i1} - M_{i2}$$

(Eq 7)

The forces acting on the joint are dominated by the internal shear force on the bone at distance L_c and L_1 from the joint, defined as the length of the implant arms as well as the corresponding length for the diaphysis of the bone with a radius of r_C and r_B respectively, and the reaction force of the joint in the plane for the static system. The frictional forces, F_f, hold the joint in place during stagnant periods. The equations for the one piece implant are shown in Eq 7-14 below

$$\sum F_x = 0 = -1[F_{shear\ 2} + V_1 + 2F_f cos\theta + F_{cx} + F_{mx} - F_{Tx} + F_{Lx}] \quad \text{(Eq 8)}$$

$$\sum F_y = 0 = -1[-F_{shear\ 1} + V_2 + 2F_f cos\theta + F_{cy} + F_{Ty} - F_{Ly} - F_{My}] \quad \text{(Eq 9)}$$

$$\sum M_c = 0 = -1[M_1 - M_2 + M_{i2} + M_{i1} - F_{shear\ 2}(L_c) - F_{shear\ 1}(L_c) - F_{Mx} r_B - F_{Tx} r_B + F_{Ty} r_c + F_{My} r_C] \quad \text{(Eq 10)}$$

$$F_{Ty} = \frac{-L_1}{L_C r_1}(M_1 - M_2) - \frac{M_{i1}}{r_1}\left(\frac{L_1}{L_C} + 2\right) - \frac{M_{i2}}{r_1}\left(\frac{L_1}{L_C} + 1\right) - 2(F_{mx} + F_{Tx}) - F_{my} \quad \text{(Eq 11)}$$

$$\sum F_x = ma = -1[F_{shear\ 2} + V_1 - F_{Tx} + F_{Lx} + F_{mx} + F_{cx} + 2F_{Ffx}] \quad \text{(Eq 12)}$$

$$\sum F_y = ma = -1[-F_{Ty} + 2F_{Ff} - F_{Ly} - F_{shear\ 1} + V_2 + F_{cy} + F_{my} + m_s g + m_s g + m_b g + m_b g] \quad \text{(Eq 13)}$$

$$\sum M_c = I\alpha = r_c\left(F_{Ty} - F_{Tx} + F_{my} - F_{mx}\right) - m_p g\left(\frac{L_1 + \Delta}{2}\right) - m_b g\left(\frac{L_1}{2}\right) + L_c(F_{shear\ 2}) + F_{shear\ 1}(L_c) - M_{i1} - M_{i2} + M_1 - M_2 \quad \text{(Eq 14)}$$

For both systems, the shear forces (determined from the analysis of the condyles) are defined as

$$F_{shear\ 1} = \frac{M_{i1}}{L_1} + \frac{r_1}{L_1}(F_{mx} + F_{Tx}) \quad \text{(Eq 15)}$$

$$F_{shear\ 2} = \frac{M_{i2}}{L_D} - \frac{r_D}{L_D}(F_{my} + F_{Ty}) \quad \text{(Eq 16)}$$

For the one-piece system, the moment of inertia is still dependent on patient geometry of both the metacarpal and phalangeal bones being examined. However, taking the differences in moment of inertia and mass to be negligible between the two cases, the examination of the forces acting on the joints provide an excellent evaluation for the recorded behavior of the one-piece joint. There will be wearing occurring on the implant due to the movement of the implant during any type of loading, as well as shear forces due to the additional moments associated with the design of the implant. Additionally, the design specifications of the one-piece implant indicate that lifting or gripping motions will be severely limited. From this evaluation, there is no joint reaction that is constant for the one-piece implant, since the arms are only held in place by frictional forces. Therefore, a more ideal joint would have geometry that more closely matches the natural joint, does not contain an internal moment that will weaken the overall design, and has a fixation that will allow for loading of the joint to occur. The comparison of the moments between the one-piece implant and the natural joint show that the forces acting on the flexor tendons differ by the associated moment of the one-piece implant multiplied by the ratio of the bone lengths and radii. By assuming that the lengths of the metacarpal and phalangeal bone segments are the same length, a value of unity, the force on the tendon is then proportional to the inverse radius of the bones.

The proposed total joint replacement design includes a tongue and groove joint to prevent lateral/medial displacement. The ridge on top prevents the hyperextension of the joint. The ideal material choice would be a metal and polymer, but could also be two metal pieces or two polymeric pieces, and in addition to the shape of the joint, reduces the friction between the two pieces, which would prevent the accumulation of metallic particulates in the surrounding tissue. The design shape and the two components allows for quick installation time. Figure 2 and 3 show the two joint components, as well as total joint assembly.

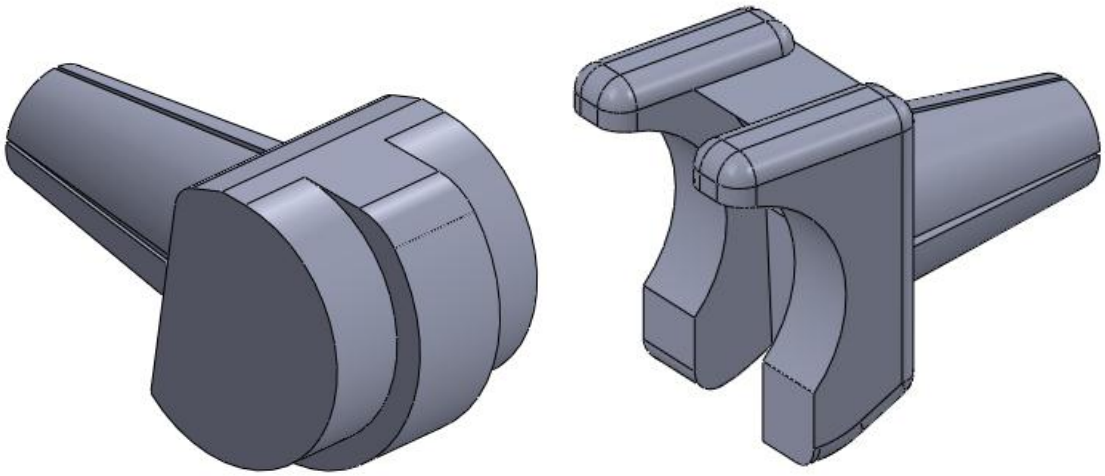

Figure 2 Both components of the total finger and toe joint replacement, shown from the front

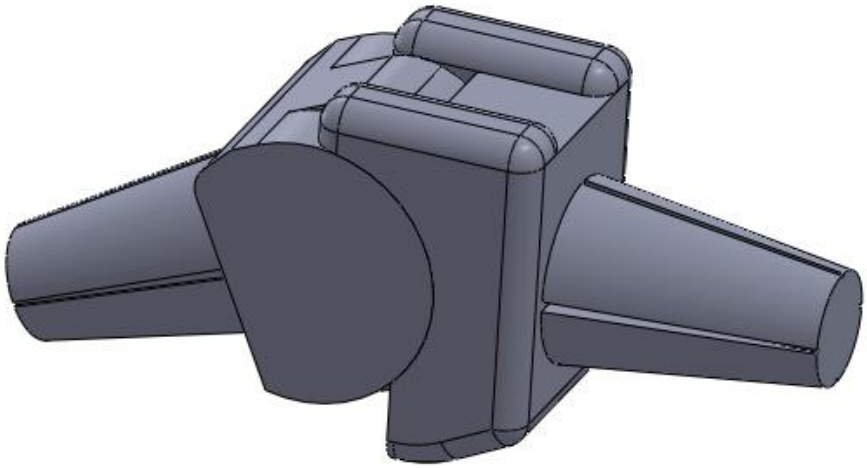

Figure 3 The total finger and toe joint replacement assembly.

The design uses current medical installation techniques to implant a TJR, with the pylon of the joint being implanted into the medullary canal. The implant is installed by creating the incision anterolateral on the metacarpal joint, moving the long extensor tendon and extensor digitorum superficialis muscles medially, in order to prevent any damage to them during the procedure.

The free body diagrams of the components are shown Figure 4.

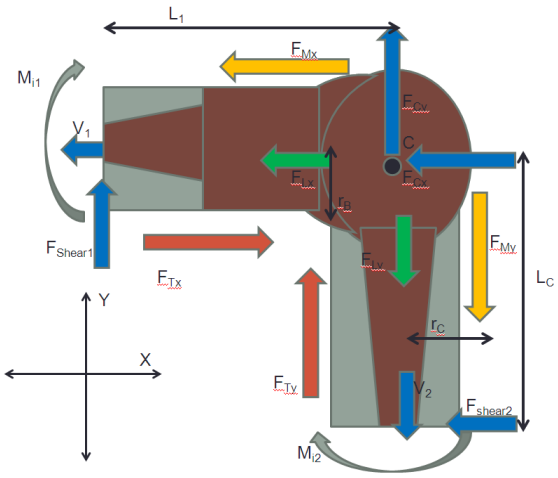

Figure 4 The free body diagrams for the proposed finger joint.

The static and dynamic equations determined from this freebody diagram are shown in Eq 17-23

$$\sum F_x = 0 = -1[F_{shear\ 2} + V_1 + F_{cx} + F_{mx} - F_{Tx} + F_{Lx}] \quad \text{(Eq 17)}$$

$$\sum F_y = 0 = F_{shear\ 1} - V_2 + F_{cy} + F_{Ty} - F_{Ly} - F_{My} \quad \text{Eq 18)}$$

$$\sum M_c = 0 = M_{i2} + M_{i1} + F_{shear\ 2}(L_c) + F_{shear\ 1}(L_1) - F_{Mx}r_B - F_{Tx}r_B + F_{Ty}r_c + F_{My}r_c \quad \text{(Eq 19)}$$

$$F_{Ty} = \frac{-M_{i1}}{r_D}\left(\frac{L_D}{L_C} + 2\right) - \frac{M_{i2}}{r_D}\left(\frac{L_D}{L_C} + 1\right) - 2(F_{mx} + F_{Tx}) - F_{my} \quad \text{(Eq 20)}$$

$$\sum F_x = ma = -1[F_{shear\ 2} + V_1 - F_{Tx} + F_{Lx} + F_{mx} + F_{jx} + F_{Ffx}] \quad \text{(Eq 21)}$$

$$\sum F_y = ma = -1[-F_{Ty} + F_{Ff} - F_{Ly} - F_{shear\ 1} + V_2 + F_{jy} + F_{my} + m_p g + m_p g + m_b g + m_b g] \quad \text{(Eq 22)}$$

$$\sum M_c = I\alpha = r_c(F_{Ty} - F_{Tx} + F_{my}) - F_{mx}(r_c + \Delta) - m_p g\left(\frac{L_1 + \Delta}{2}\right) - m_b g\left(\frac{L_1}{2}\right) + L_c(F_{shear\ 2}) + F_{shear\ 1}(L_c) - M_{i1} - M_{i2}$$

(Eq 23)

where the shear forces are defined as shown in Eq 15 and 16.

The proposed TJR has the same static analysis as the natural joint. In the dynamic analysis, Δ is the length between the center of mass for the joint arms and the center of mass for the bone shaft. The differences between the dynamic analysis of the natural and proposed joints are the moments of inertia (*I*) and masses. *I* is not calculated due to difficulties in accurately using the complex organic shapes and surfaces of the joints. There is no internal moment with the proposed implant, and the fixation of the condyles of the joint allow for the joint reaction forces, which would provide the patient with a point to apply force around. The surgical procedure for implating such an orthopedic device involves bonding the pylons to the bones using PMMA (polymethyl methylacrylate), which removes all frictional forces from this scenario. The result of this would be the patient would regain functionality of the joint in all loading applications, including gripping and lifting of objects.

Computational Modeling and Simulation

The joint was designed in Solidworks, and a three dimension theoretical model was tested within the software, using the SimulationXpress Analysis package (standard), then within ANSYS Multiphysics software. Ultra high molecular weight polyethylene (UHMWPE) and solution treated titanium (Ti) alloy (6Ti-4Al-W) were used as the materials in the analysis, due to their high mechanical strength and compatibility properties [20-22, 24-26]. Any risks associated with Ti alloy particles are rendered negligible through the use of UHMWPE as the surface against which it articulates. As demonstrated by a general adhesive wearing equation (Eq 24), the particles produced will be of the softer material (the polymer).

$$V = \frac{k * F_N * x}{3 * \rho_{soft}} \qquad \text{(Eq 24)}$$

V is the total adhesive wear volume of the material, *k* is Archard's coefficient (which varies based upon surface conditions and the material choice), F_N is the force applied, *x* is the sliding distance, and ρ_{soft} is the Vickers hardness value of the softer material. From this trend, without considering the surface condition, the majority of the wearing will be attributed to the polymeric material. [22]

Preliminary analysis of the joint demonstrated that acceptable allocations of materials include: both components being Ti alloy or UHMWPE, or the distal cup being Ti alloy and the proximal male end being UHMWPE.

The assembly was tested, as well as the individual components. The individual components had stresses on the orders of 3 and 4 MPa before deforming less than 1.0 mm for loads of 10 N, a load similar to that of griping a ball or a door knob. For this reason, the entire assembly simulation results are defined as the maximum acceptable stress for the joint. Further analysis was done using force allocation similar to the free body diagrams, with a force pushing the components together, a lesser force pulling them apart on the posterior (top) of the assembly, and a third force creating movement of the male end on the female end.

RESULTS AND DISCUSSION

Figure 5 shows the results for evaluations with forces of magnitudes between 1 N and 10 N.

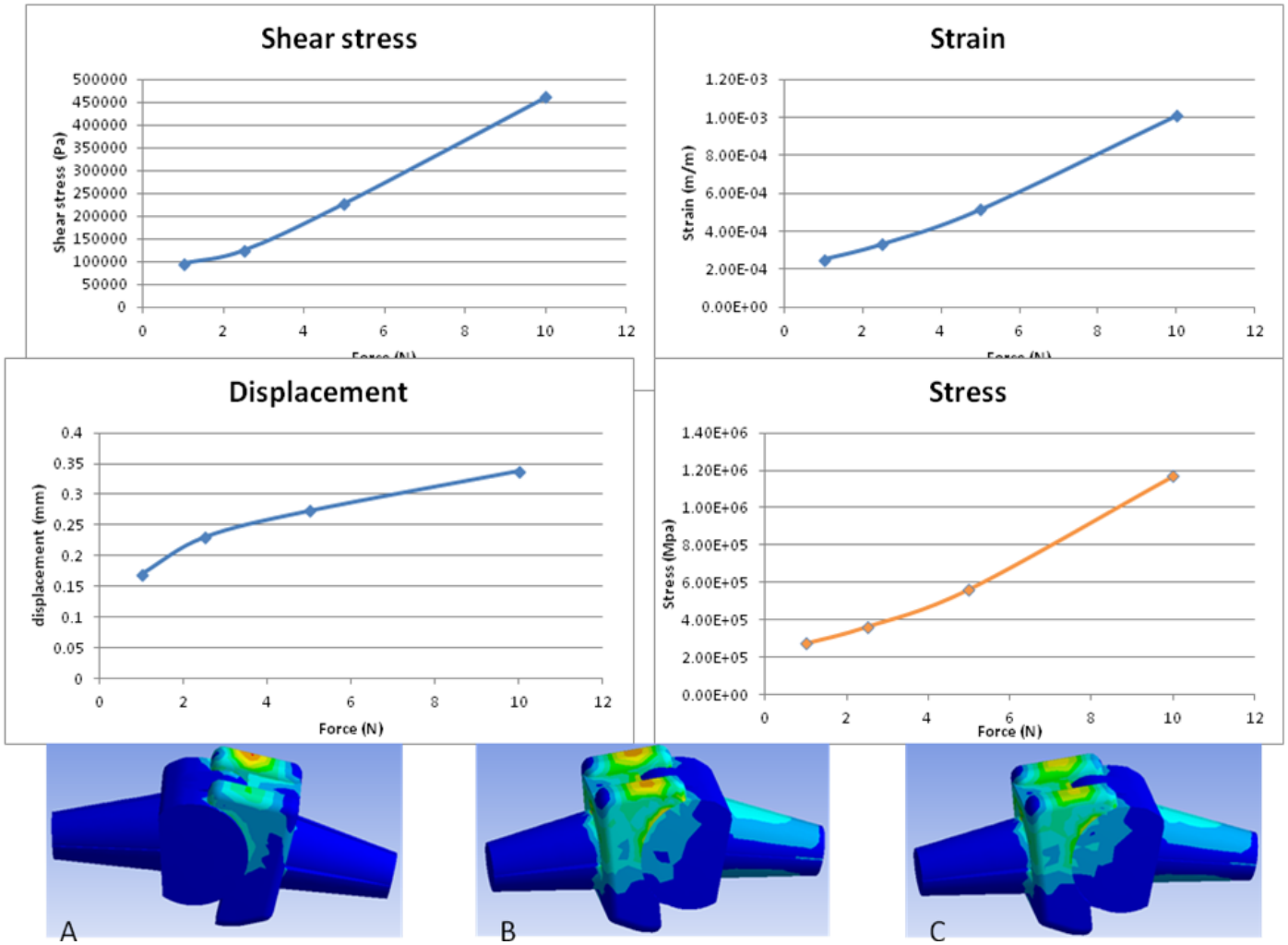

Figure 5 The shear stress, strain, displacement and stress curves for the total joint assembly at loads between 1 and 10 N. Images A-C below show the location of the stress at 1 N (A), 5 N (B) and 10 N(C).

The key locations for the stress on the joint are at the connection between the pylons and the joint bodies, the contacting surfaces, and the top of the socket joint, as shown in the images of Figure 5. The allocation of forces from these loading simulations demonstrates that the force is transferred through the ball joint into the socket. For this reason, the socket is recommended to be metallic, and the ball polymeric in terms of material selection, in order to minimize wearing and deformation of the joint under day-to-day loading.

CONCLUSIONS

Theoretical testing of the joint demonstrated a high tolerance for applied stresses from daily activity involving the joint. The assigned forces were applied from assumptions made about basic tasks involving the joint, such as force applied parallel to the digit with the TJR. The second major force application was perpendicular to the fully extended digit. Oblique forces were not tested.

One portion of the study not yet performed is the stress and displacement distribution attributed to the physical characteristics of the joint. It is possible that as the radii of the joint head decreases, the force distribution across the surface will be decreased. The length of the pylons or the radii of the tongue may also affect this. This study will be crucial to comparing the joint performance with other designs due the variation in sizes between patients and even the joints on a single patient.

It is very plausible that this design can be used in total finger and toe joint replacement surgeries. Future work will include cadaver implantation of varying joint sizes, to determine the range of difficulty for surgeons and patients in terms of time of implantation, biomechanical functionality, and tissue destruction. Additionally, physical testing will be performed to corroborate the theoretical models, with the selected material of UHMWPE used. More complete analysis of the system is ongoing, in order to incorporate both the bone tissues present and the bone cement used. [27, 28]

The current prototype is not being suitable for physical stress testing, due to the mechanical properties of the prototyping plastic and the method used in creating the prototype. Mechanical testing will be done to compare the differences between titanium alloy and UHMWPE in terms of yield limit, deformation and wearing characteristics.

ACKNOWLEDGMENTS

I would like to acknowledge Dr. Ha Van Vo, without whom this study would not have been possible. Additionally, I would like to thank Jeff Cope of Central Georgia Technical College for the usage of the rapid prototyper in producing our components.

REFERENCES

1. Ash HE, Unsworth A. Design of a surface replacement prosthesis for the proximal interphalangeal joint. Proc Inst Mech Eng H. 2000;214(2):151-63.
2. Morris, John MD. Joint Replacement Surgery of the Hand. MedicineNet.com. 2008.
3. Watts, A.C.; Trail, I.A. Anatomical Small Joint replacement in the hand. The Journal of bone and joint surgery, 2011.
4. A.B. Ann. Finger joint replacement by silicone rubber implants and the concept of implant fixation by encapsulation. Swanson, Rheum. Dis. 1969. Vol 28, Supplement p 47-55.
5. Henry Gray Gray's Anatomy.. Philadelphia, PA. T. Pickering Pick. 1974
6. Netter, F. Saunders. Atlas of Human Anatomy 5th edition. Elsevier, Philadelphia, PA. 2011.
7. Hannon, P; Knapp, K. Forensic Biomechanics. Lawyers and Judges Publishing Company, Inc.Tucson, AZ. 2008
8. Whting, W; Zernicke, R. Biomechanics of Musculoskeletal Injury. Human Kinetics, Champaign, IL 2008.
9. Brinckmann, P; Froin, W; Leivseth, G. Musculoskeletal Biomechanics. Stuttgart, Germany. Georg Thieme Verlag. 2000.
10. Merolli, A. Prostheses for the Joints of the Hand, Biomaterials in Hand Surgery. Springer Verlag Italia 2009: Assago, Italy. P47-69.
11. Sweets, T; Stern, P. Pyrolytic Carbon Resurfacing Arthroplasty for Osteoarthritis of the Proximal Interphalangeal Joint of the Finger. J Bone Joint Surg Am. 2011;93:1417-25
12. . Joyce, T. Causes of Failure in Flexible Metacarpophalangeal ProsthesesSpringer Verlag Italia 2009: Assago, Italy. P69-80.
13. Catalano, F. Prosthetic Surgery of Metacarpophalangeal Joints in Rheumatoid Patients: an Open Problem. Springer Verlag Italia 2009: Assago, Italy. P83-91.
14. Merolli, A. Requirements for a Metacarpophalangeal Joint Prosthesis for Rheumatoid Patients and Suggestions for Design. Springer Verlag Italia 2009: Assago, Italy. P95-105
15. Kay, A; Jeffs, J; Scott, J. Experience with silastic prostheses in the rheumatoid hand. Annals of the Rheumatic Diseases, 1978, 37, 255-258
16. Watts, A; Trial, I. Focus On: Anatomical Small Joint Replacement in the Hand. THE JOURNAL OF BONE AND JOINT SURGERY
17. Artificial joints for the hand and wrist. Harvard Medical School newsletter, Harvard Health Publications, 2008.
18. Murray, Peter. Surface replacement arthroplasty of the proximal interphalangeal joint. Course lecture, Department of Orthopedic Surgery, Mayo Clinic. February 2007.

19. Peter M. Murray. New-Generation Implant Arthroplasties of the Finger Joints, American Academy of Orthopedic Surgeons. 2003.
20. Ratner, B; Hoffman, A; Schoen, F; Lemons, J. Biomaterials Science, An Introduction to Materials in Medicine, 2nd Edition. Elsevier Academic Press. San Diego, California, 2004
21. Tranquilli, P; Merolli, A. Fundamentals of Biomaterials. Biomaterials in Hand Surgery. Pg 1-12.
22. Pruitt, L; Chakravartula, C. Mechanics of Biomaterials: Fundamental Principles for Implant Design. Cambridge University Press, Cambridge UK, 2011.
23. Swanson, A. Wright. Swanson: flexible finger joint implant. Medical Technology, Inc., Arlington, TN, 2003.
24. Hallab, N; Urban, R; Jacobs, J. Corrosion and Biocompatibility of Orthopedic Implants. Biomaterials in Orthopedics. Edited by Michael Yaszemski, 2004, New York, New York, pg 63-91.
25. Beil, J; Heller, J; Andriano, K. Rational Design of Absorbable Polymers for Orthopedic Repair. Biomaterials in Orthopedics. Edited by Michael Yaszemski, 2004, New York, New York, pg 149- 157
26. Kahyaoglu, O; Unal, H.Friction and wear behaviors of medical grade UHMWPE at dry and lubricated conditions. Inter. J Phys Sci Vol.7(16) pp 2478-2485, April 2012
27. Anderson, A; Dallmier, A; Chudzik, S; Duran, L , et al. Technologies for the Surface Modification of Biomaterials. Biomaterials in Orthopedics. Edited by Michael Yaszemski, 2004, New York, New York, pg 93-148.
28. Serbetci, K; Hasirci, N. Recent Developments in Bone Cement. Biomaterials in Orthopedics. Edited by Michael Yaszemski, 2004, New York, New York, pg 241-286.

BIOGRAPHICAL INFORMATION

Andrew Weems

Andrew Weems is a Masters student at Mercer University, specializing in Biomedical Engineering. The paper submitted is in conjunction with the research being done on his thesis, which is to develop a total joint replacement for metacarpophalangeal, metatarsolphalangeal and interphalangeal joints. Other research projects include the development of total joint replacements for the elbow and ankle joints.